Electronic Supplementary Material (ESI) for ChemComm.

Supporting Information

N,*N*-diethyl-3-methylbenzamide (DEET) acts as a metal-organic framework synthesis solvent with phase-directing capabilities

Ryan A. Dodson,[†] Andre P. Kalenak,[†] Derek R. Du Bois,[†] Sasha L. Gill-Ljunghammer,[†] and Adam J. Matzger[,†,‡]*

[†]Department of Chemistry and [‡]Macromolecular Science and Engineering Program, University of Michigan, 930 North University Avenue, Ann Arbor, Michigan 48109-1055, United States

Table of Contents:

1. Reagents

Zinc perchlorate hexahydrate (Alfa Aesar, reagent grade), aluminum nitrate nonahydrate (Fisher, certified ACS grade), aluminum chloride hexahydrate (Sigma, 99%), cupric nitrate hemipentahydrate (Fisher, certified ACS grade), zirconium(IV) chloride (Strem, sublimed grade), 1,4-benzenedicarboxylic acid (H_2bdc, Fisher Scientific, 98%), 2-aminoterephthalic acid (H_2bdc-NH_2, Sigma-Aldrich, 99%), 2,6-naphthalenedicarboxylic acid (H_2ndc, TCI America, 98%), 4,4'-biphenyldicarboxylic acid (H_2bpdc, Acros Organics, 98%), 1,3,5-benzenetricarboxylic acid (H_3btc, TCI America, 98%), 1,3,5-tri(4-carboxyphenyl)benzene (H_3btb, Alfa Aesar, 97%), imidazole (Him, Aldrich, 99%), 2-methylimidazole (Hmim, Acros Organics, 99%), 2-nitroimidazole (Hnim, Oakwood Chemical, 98%), 4,4'-bipyridine (4,4'-bpy, Acros Organics, 98%), hydrochloric acid (Fisher Scientific, certified ACS plus), acetic acid (Fisher Scientific, glacial, certified ACS plus), nitric acid (Fisher Scientific, certified ACS plus), and fluoroboric acid (Acros Organics, 50 wt% solution in water) were used as received. Zinc nitrate hexahydrate (Fisher Scientific, ACS grade) was partially dehydrated by room temperature evacuation (~16 hr, <0.01 Torr) to yield zinc nitrate tetrahydrate (verified by thermogravimetric analysis). DCl in D_2O (Sigma Aldrich, 99+% atom D) and DMSO-d_6 (Acros Organics, 99.5+% atom D) were used for ^{1}H-NMR experiments. *N*,*N*-diethyl-3-methylbenzamide (DEET, Acros Organics, 98%), hexane (Fisher Scientific, anhydrous), methylene chloride (CH_2Cl_2, Fisher scientific, HPLC grade), *N*-methylpyrrolidone (Sigma Aldrich, 99.5%), and *N*,*N*-dimethylformamide (DMF, Fisher Scientific, 99.5%) were stored over activated 4 Å molecular sieves to minimize water content. The dryness of these solvents was monitored by Karl Fischer titration (<10 ppm H_2O). *N*,*N*-Diethylformamide (DEF, TCI America, >99.0%) was purified by storage on activated charcoal for ~1 month followed by removal of impurities via silica gel column.

2. Syntheses

MOF syntheses were generally performed with minimal modification relative to literature-reported protocols with the exception of solvent substitution. When syntheses called for zinc nitrate hexahydrate as a zinc source, the tetrahydrate was substituted. All MOF syntheses were also performed in the original formamide solvent to ensure the efficacy of these procedures. Unless otherwise stated, syntheses were performed in 20 mL vials with Teflon-lined caps. The specific syntheses performed were as follows attempting to make the named MOF:

<u>Zn MOFs</u>

MOF-5.[1] $Zn(NO_3)_2{\cdot}4H_2O$ (360.0 mg, 1.377 mmol) and H_2bdc (60.0 mg, 0.361 mmol) were dissolved in DEET (10 mL). The reaction was performed at 100 °C for 1 day.

IRMOF-3.[2] $Zn(NO_3)_2{\cdot}4H_2O$ (333.3 mg, 1.275 mmol) and H_2bdc-NH_2 (83.3 mg, 0.460 mmol) were dissolved in DEET (10 mL). The reaction was performed at 100 °C for 3 days.

UMCM-1.[3] $Zn(NO_3)_2{\cdot}4H_2O$ (566.6 mg, 2.167 mmol), H_2bdc (90.0 mg, 0.542 mmol), and H_3btb (213.4 mg, 0.487 mmol) were dissolved in 20 mL DEET. The reaction was performed at 85 °C for 2 days.

UMCM-9.[4] $Zn(NO_3)_2{\cdot}4H_2O$ (216.0 mg, 0.826 mmol), H_2ndc (29.1 mg, 0.135 mmol), and H_2bpdc (36.8 mg, 0.152 mmol) were dissolved in DEET (20 mL). The reaction was performed at 85 °C for 7 days.

MOF-177.[5] $Zn(NO_3)_2 \cdot 4H_2O$ (164.7 mg, 0.630 mmol) and H_3btb (39.5 mg, 0.090 mmol) were dissolved in DEET (10 mL). The reaction was performed at 85 °C for 4 days.

Zn-HKUST-1.[6] $Zn(NO_3)_2 \cdot 4H_2O$ (153.6 mg, 0.587 mmol) and H_3btc (35.6 mg, 0.169 mmol) were dissolved in DEET (10 mL). The reaction was performed at 85 °C for 16 hours.

ZIF-8.[7] $Zn(NO_3)_2 \cdot 4H_2O$ (210.0 mg, 0.803 mmol) and Hmim (60.0 mg, 0.731 mmol) were dissolved in DEET (18 mL). The reaction was performed at 140 °C for 1 day in a Teflon-lined stainless-steel autoclave.

ZIF-70.[8] $Zn(NO_3)_2 \cdot 4H_2O$ (209.2 mg, 0.800 mmol), Hnim (113.1 mg, 1.000 mmol), and Him (68.1 mg, 1.000 mmol) were dissolved in DEET (14 mL). The reaction was performed at 110 °C for 4 days.

FJI-1.[9] $Zn(ClO_4)_2 \cdot 6H_2O$ (223.0 mg, 0.599 mmol), H_3btb (175.0 mg, 0.399 mmol), and 4,4'-bpy (47.0 mg, 0.301 mmol) were dissolved in DEET (10 mL) along with 0.1 mL fluoroboric acid. The reaction was performed at 85 °C for 3 days.

Cu MOFs

HKUST-1.[10] $Cu(NO_3)_2 \cdot 2.5H_2O$ (400.0 mg, 1.720 mmol) and H_3btc (200 mg, 0.952 mmol) were dissolved in DEET (10 mL) along with a drop of concentrated HCl. The reaction was performed at 85 °C for 16 hours.

Cu-MOF-2.[11] $Cu(NO_3)_2 \cdot 2.5H_2O$ (121.0 mg, 0.520 mmol) and H_2bdc (83.2 mg, 0.501 mmol) were dissolved in DEET (10 mL). The reaction was performed at 110 °C for 36 hours.

Zr MOFs

UiO-66.[12] $ZrCl_4$ (83.3 mg, 0.358 mmol) and H_2bdc (82.0 mg, 0.494 mmol) were dissolved in DEET (10 mL) along with 0.67 mL HCl. The reaction was performed at 85 °C for 16 hours.

DUT-52.[13] $ZrCl_4$ (115.0 mg, 0.493 mmol) and H_2ndc (108.0 mg, 0.500 mmol) were dissolved in DEET (10 mL) along with 1.5 mL acetic acid. The reaction was performed at 85 °C for 16 hours.

UiO-67.[12] $ZrCl_4$ (44.7 mg, 0.192 mmol) and H_2bpdc (60.0 mg, 0.248 mmol) were dissolved in DEET (10 mL) along with 0.33 mL HCl. The reaction was performed at 85 °C for 16 hours.

Al MOFs

MIL-53(Al).[14] $Al(NO_3)_2 \cdot 9H_2O$ (96.3 mg, 0.257 mmol) and H_2bdc (96.0 mg, 0.578 mmol) were dissolved in DEET (10 mL). The reaction was performed at 120 °C for 3 days.

MOF-519.[15] $AlCl_3 \cdot 6H_2O$ (50.6 mg, 0.135 mmol) was dissolved in DEET (5 mL) and mixed with a 5 mL H_3btb (109.0 mg, 0.249 mmol) DEET solution along with 0.68 mL HNO_3. The reaction was performed at 150 °C for 3 days in a Teflon-lined stainless-steel autoclave.

3. Powder X-ray diffraction

Room-temperature powder X-ray diffraction was performed on a PANalytical Empyrean diffractometer in Bragg–Brentano geometry (Cu K_α radiation, 45 kV, and 40 mA). The incident beam was equipped with a Bragg–BrentanoHD X-ray optic using fixed slits/soller slits. X-ray detection was accomplished with a silicon-based linear position sensitive X'Celerator Scientific detector operating in 1D scanning mode. When necessary (MOF-5, UMCM-1, UMCM-9, MOF-177, Zn/btc), samples were finely ground to minimize preferred orientation and packed in the depression of a glass slide. Patterns were collected between 3 – 80 °2Θ, with a scan rate of 0.008 ° and 20 seconds per step. Powder X-ray diffractograms for DEET-synthesized MOFs along with diffraction patterns calculated from crystal structures are given in Figures S1-S9. As needed, experimental patterns of materials created using the original synthesis solvent are given for comparison.

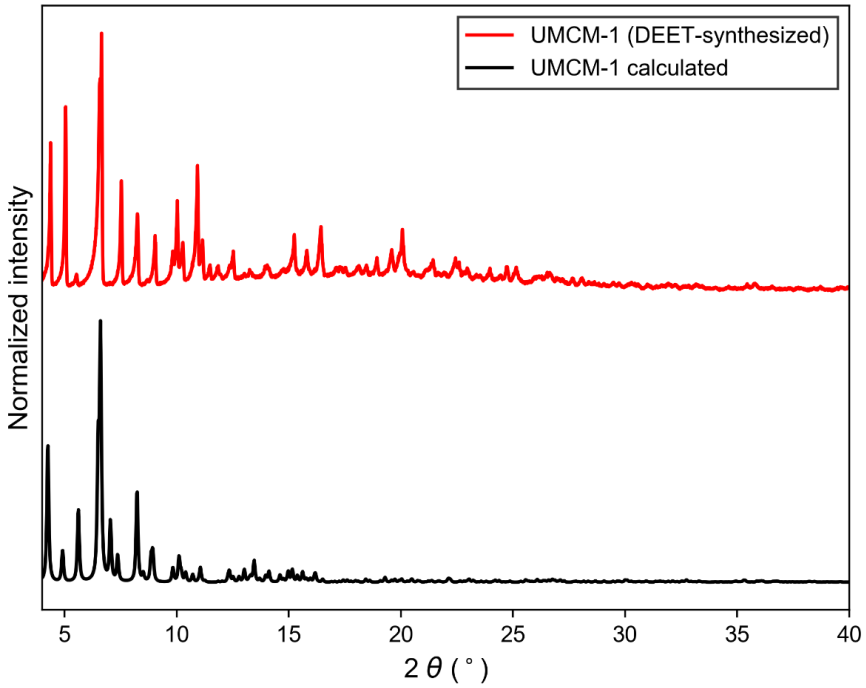

Figure S1. PXRD pattern of DEET-synthesized UMCM-1 (above) and calculated PXRD pattern for UMCM-1 (below).

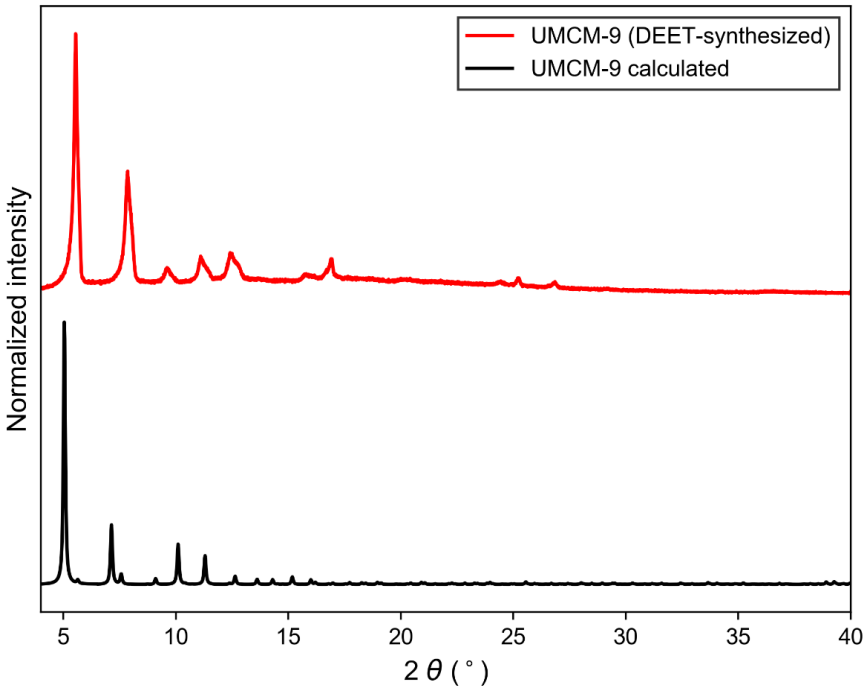

Figure S2. PXRD pattern of DEET-synthesized UMCM-9 (above) and calculated PXRD pattern for UMCM-9 (below). The broader peaks in the experimental pattern are consistent with previously reported UMCM-9 patterns, and can be attributed to the inherent structural disorder in the MOF system.[4]

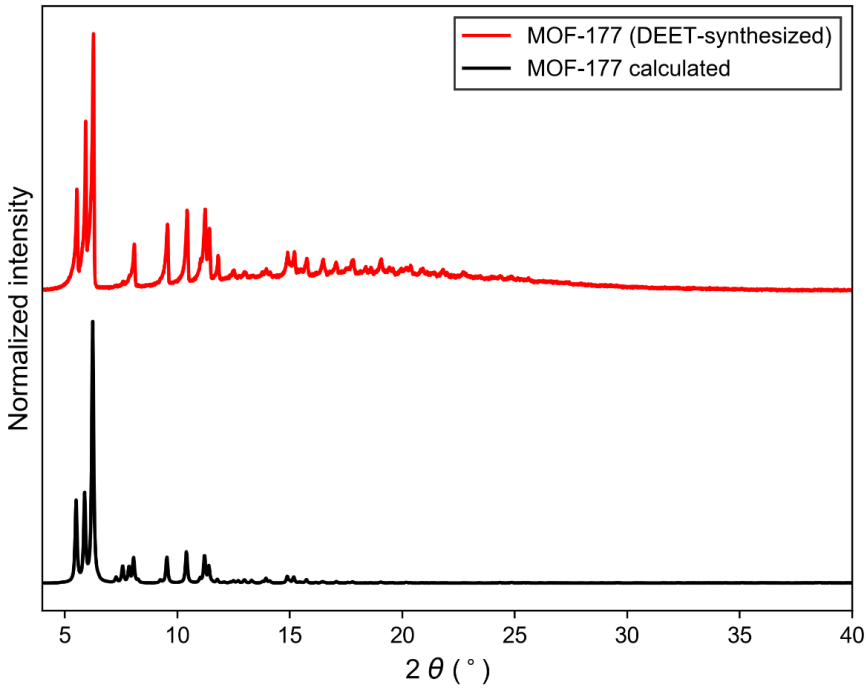

Figure S3. PXRD pattern of DEET-synthesized MOF-177 (above) and calculated PXRD pattern for MOF-177 (below).

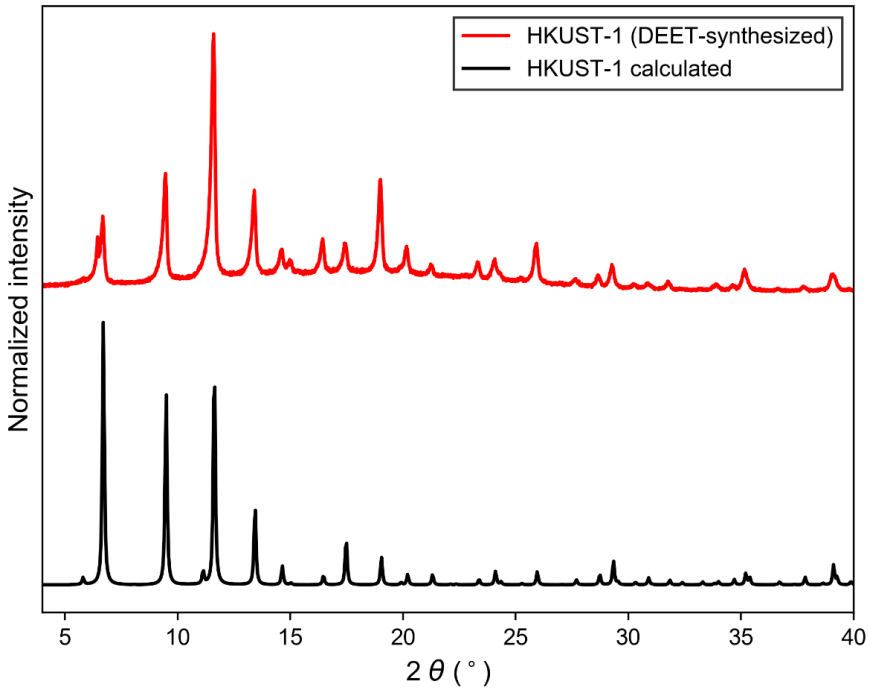

Figure S4. PXRD pattern of DEET-synthesized HKUST-1 (above) and calculated PXRD pattern for HKUST-1 (below).

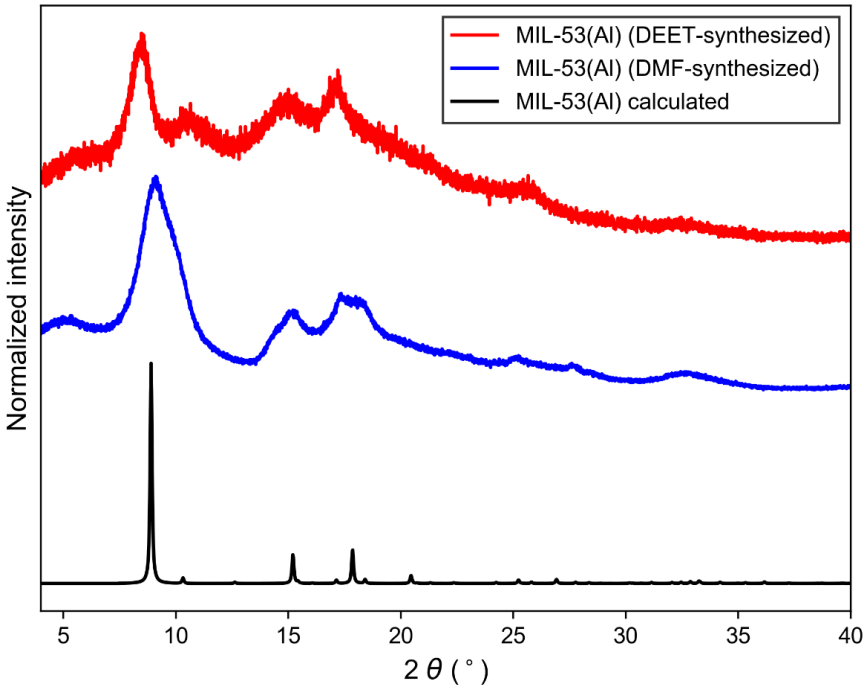

Figure S5. PXRD pattern of DEET-synthesized MIL-53(Al) (above), DMF-synthesized MIL-53(Al) (middle), and calculated PXRD pattern for MIL-53(Al) (below). The broad peaks and high background in both experimental patterns suggest that this synthesis (regardless of solvent) yields relatively small crystalline domains and/or a substantial fraction of amorphous material.

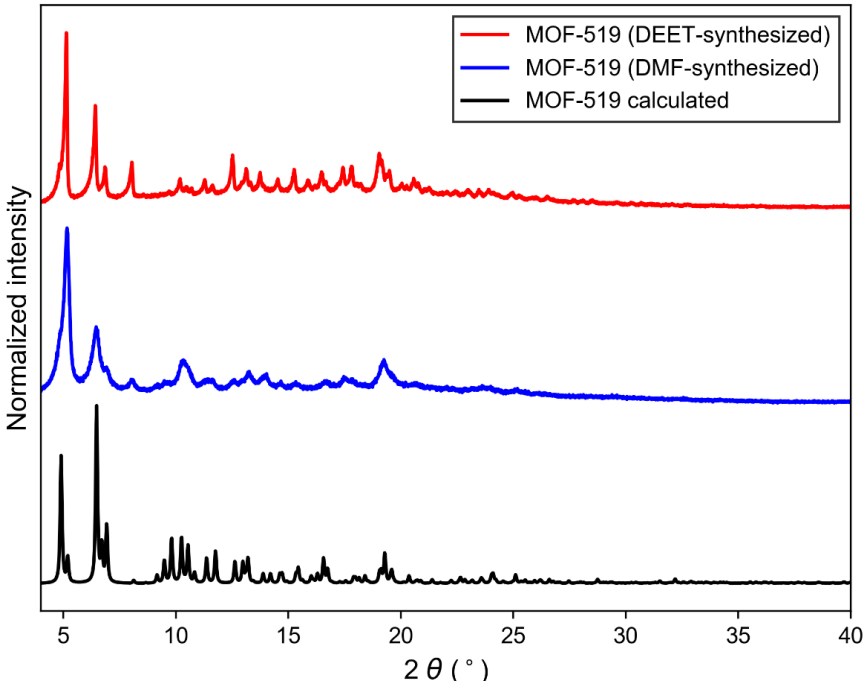

Figure S6. PXRD pattern of DEET-synthesized MOF-519 (above), DMF-synthesized MOF-519 (middle), and calculated PXRD pattern for MOF-519 (below).

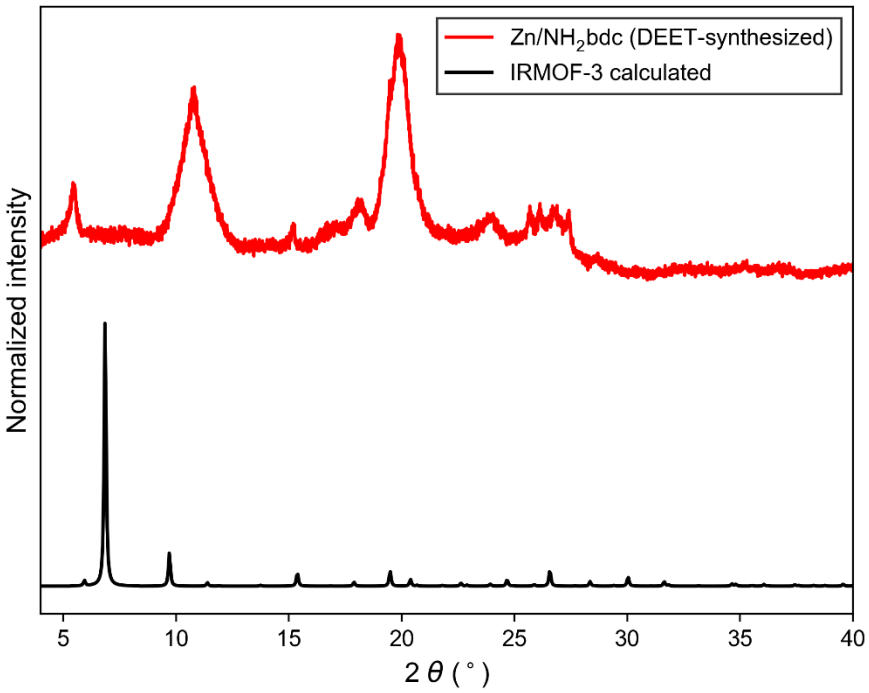

Figure S7. PXRD pattern of DEET-synthesized Zn/NH_2-bdc (above) and calculated PXRD pattern for IRMOF-3 (below).

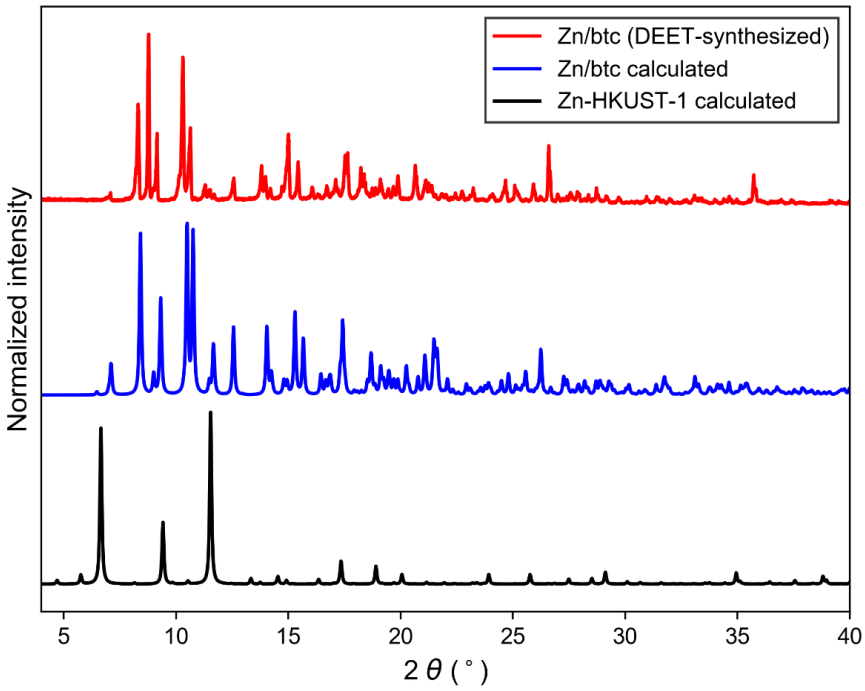

Figure S8. PXRD pattern of DEET-synthesized Zn/btc (above), calculated PXRD pattern for that phase (middle), and calculated PXRD pattern for Zn-HKUST-1 (below).

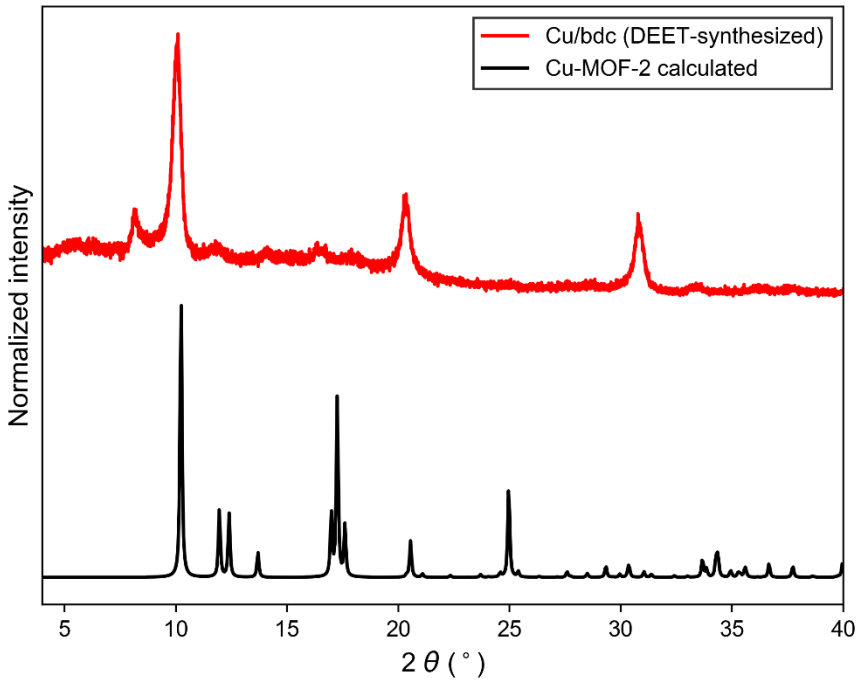

Figure S9. PXRD pattern of DEET-synthesized Cu/bdc (above) and calculated PXRD pattern for Cu-MOF-2 (below).

4. Vapor pressure measurements

Vapor pressures and heats of vaporization were determined using the Knudsen effusion method. Briefly, each sample was placed in an aluminum DSC pan which was then sealed with a hermetic lid containing a 75 μm-diameter laser-drilled hole (TA Instruments). This pan was then loaded into a TA Q50 thermogravimetric analyzer, and weight loss was recorded at constant temperature. Experiments were performed in triplicate. Temperature-dependent vapor pressures were calculated from measured mass loss rates using the Langmuir equation (eq. 1).[16]

$$p = \left(\frac{\Delta m}{\Delta t}\right)\left(\frac{1}{A}\right)\left(\frac{2\pi RT}{M}\right)^{1/2} \quad (1)$$

Where p is the equilibrium vapor pressure (Pa), $\Delta m/\Delta t$ is mass loss rate (kg s^{-1}), A is the pinhole area (m^2), R is the ideal gas constant (8.314 m^3 Pa mol^{-1} K^{-1}), T is the temperature (K), and M is the molar molecular weight of the volatile species (kg mol^{-1}).

An example calculation is given below:

$\Delta m/\Delta t = 0.00356$ mg $min^{-1} = 5.93 \times 10^{-11}$ kg s^{-1}

$T = 175.00$ °C $= 448.15$ K

$A = \pi \times (75\ \mu m / 2)^2 = 4.42 \times 10^{-9}\ m^2$

$M = 0.19127$ kg mol^{-1}

$$p = (5.93 \times 10^{-11}\ \text{kg}\ s^{-1})\left(\frac{1}{4.42 \times 10^{-9} m^2}\right)\left(\frac{2\pi \times 8.314\ m^3\ Pa\ mol^{-1}K^{-1} \times 448.15\ K}{0.19127\ kg\ mol^{-1}}\right)^{1/2}$$

$$p = (1.34 \times 10^{-2}\ \text{kg}\ m^2\ s^{-1})(1.223 \times 10^5\ m^3\ Pa\ kg^{-1})^{1/2}$$

$$p = (1.34 \times 10^{-2}\ \text{kg}\ m^2\ s^{-1})(1.223 \times 10^5\ m^2\ s^{-2})^{1/2}$$

$$p = (1.34 \times 10^{-2}\ \text{kg}\ m^2\ s^{-1})(349.9\ m\ s^{-1})$$

$$p = 4.70\ \text{Pa}$$

Vapor pressures were then used along with the Clausius–Clapeyron relation (eq. 2) to extrapolate the 37 °C vapor pressure of DEET in bulk as well as in MOF-5.

$$ln(P) = \frac{-\Delta H_{vap}}{R}\left(\frac{1}{T}\right) + C \quad (2)$$

The Clausius–Clapeyron plot for bulk DEET is given in Figure S10.

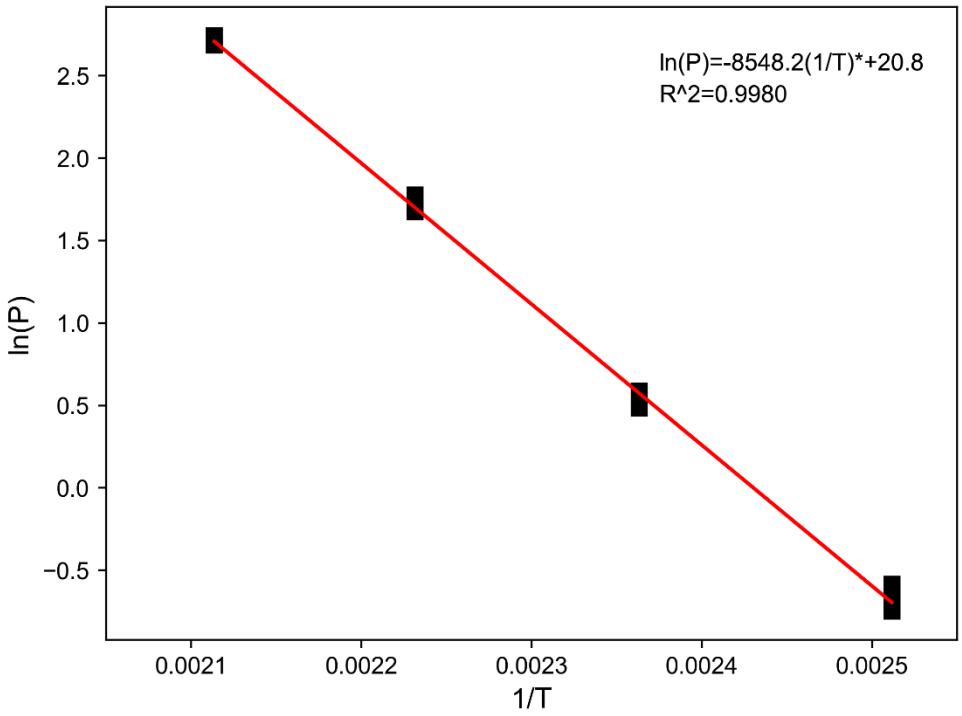

Figure S10. Clausius–Clapeyron plot for bulk DEET.

The same procedure was then used for evaluation of DEET vapor pressure depression in MOF-5. Generally, isothermal mass loss vs. time plots showed two distinct stages. In the first stage, mass loss proceeded at the same rate as bulk DEET at the same temperature. After this first stage, a sharp kink in the data was generally observed, followed by a second stage characterized by significantly slower mass loss (~1-10% vs. bulk, temperature dependent). Trials in which the mass loss rate in the first phase did not correspond with the bulk mass loss rate, or in which a sharp transition between the two phases was not observed, were not used for vapor pressure calculations. These two types of evaporation data were noted to occur when adequate space was not left between the sample and the pinhole lid, and when the pan was not properly sealed.

Vapor pressure measurements were made in triplicate at 125, 150, 175, and 200 °C. Attempts to perform lower temperature measurements resulted in mass loss too slow to accurately measure with this method using our instrumentation. The Clausius–Clapeyron plot for DEET in MOF-5 is given in Figure S11, with measured evaporation rates for bulk DEET and DEET in MOF-5 given in Tables S1 and S2, respectively.

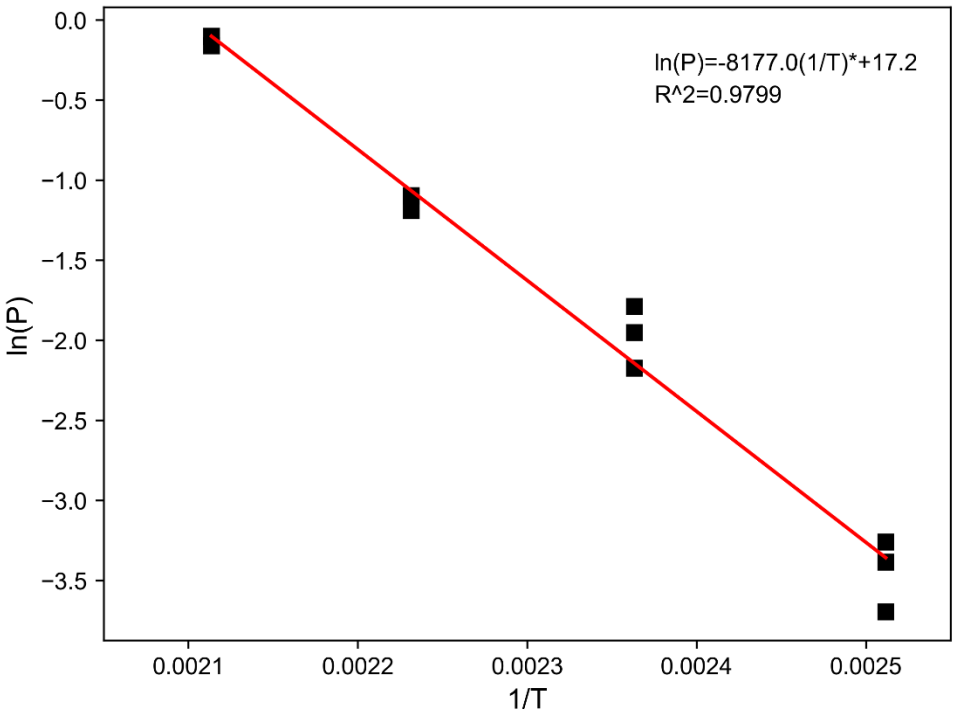

Figure S11. Clausius–Clapeyron plot for DEET in MOF-5.

Table S1. Evaporation rate data, calculated vapor pressure, and 1/T and ln(P) values used for bulk DEET vapor pressure characterization.

Temperature (°C)	Mass change (mg min^{-1})	Evaporation rate (g sec^{-1})	P_{vap} (Pa)	1/T (K^{-1})	ln(P)
125	-4.4765E-04	7.4608E-09	5.5690E-01	2.5116E-03	-5.8538E-01
125	-4.0453E-04	6.7422E-09	5.0326E-01	2.5116E-03	-6.8665E-01
125	-3.8092E-04	6.3486E-09	4.7388E-01	2.5116E-03	-7.4680E-01
150	-1.2658E-03	2.1097E-08	1.6235E+00	2.3632E-03	4.8455E-01
150	-1.3121E-03	2.1869E-08	1.6828E+00	2.3632E-03	5.2048E-01
150	-1.4027E-03	2.3379E-08	1.7990E+00	2.3632E-03	5.8726E-01
175	-4.0390E-03	6.7317E-08	5.3310E+00	2.2314E-03	1.6735E+00
175	-4.4700E-03	7.4500E-08	5.8998E+00	2.2314E-03	1.7749E+00
175	-4.1581E-03	6.9302E-08	5.4881E+00	2.2314E-03	1.7026E+00
200	-1.0832E-02	1.8053E-07	1.4690E+01	2.1135E-03	2.6872E+00
200	-1.1448E-02	1.9080E-07	1.5526E+01	2.1135E-03	2.7425E+00
200	-1.0741E-02	1.7902E-07	1.4567E+01	2.1135E-03	2.6787E+00

Table S2. Evaporation rate data, calculated vapor pressure, and 1/T and ln(P) values used for DEET in MOF-5 vapor pressure characterization.

Temperature (°C)	Mass change (mg min^{-1})	Evaporation rate (g sec^{-1})	P_{vap} (Pa)	1/T (K^{-1})	ln(P)
125	-3.0906E-05	5.1510E-10	3.8449E-02	2.5116E-03	-3.2584E+00
125	-2.7280E-05	4.5467E-10	3.3938E-02	2.5116E-03	-3.3832E+00
125	-2.0018E-05	3.3363E-10	2.4903E-02	2.5116E-03	-3.6928E+00
150	-1.1085E-04	1.8476E-09	1.4217E-01	2.3632E-03	-1.9507E+00
150	-8.8712E-05	1.4785E-09	1.1377E-01	2.3632E-03	-2.1735E+00
150	-1.3040E-04	2.1733E-09	1.6724E-01	2.3632E-03	-1.7883E+00
175	-2.3089E-04	3.8482E-09	3.0475E-01	2.2314E-03	-1.1883E+00
175	-2.5278E-04	4.2130E-09	3.3364E-01	2.2314E-03	-1.0977E+00
175	-2.5344E-04	4.2239E-09	3.3450E-01	2.2314E-03	-1.0951E+00
200	-6.6685E-04	1.1114E-08	9.0437E-01	2.1135E-03	-1.0052E-01
200	-6.2856E-04	1.0476E-08	8.5244E-01	2.1135E-03	-1.5965E-01
200	-6.0063E-04	1.0011E-08	8.1456E-01	2.1135E-03	-2.0510E-01

From these data, the vapor pressure at 37 °C for DEET in MOF-5 is extrapolated to be ~9% of that of the bulk liquid (1.05×10^{-4} Pa vs. 1.15×10^{-3} Pa).

5. Surface area determination

A ~30 mg sample of MOF-5 synthesized in DEET (per the first reaction described in Section S2) was washed 3× each with DMF, CH_2Cl_2, and hexane (~20 mL per wash, 15 minutes between washes). The sample was then evacuated under high vacuum (<0.001 Torr) for 16 hours prior to analysis. Sample surface area was calculated using the BET method from N_2 sorption isotherms measured on a Quantachrome NOVA 4200 gas sorption analyzer. The isotherm (Figure S12) and BET fit (Figure S13) are presented below. The surface area for the MOF-5 sample was calculated to be 3255 m^2 g^{-1}.

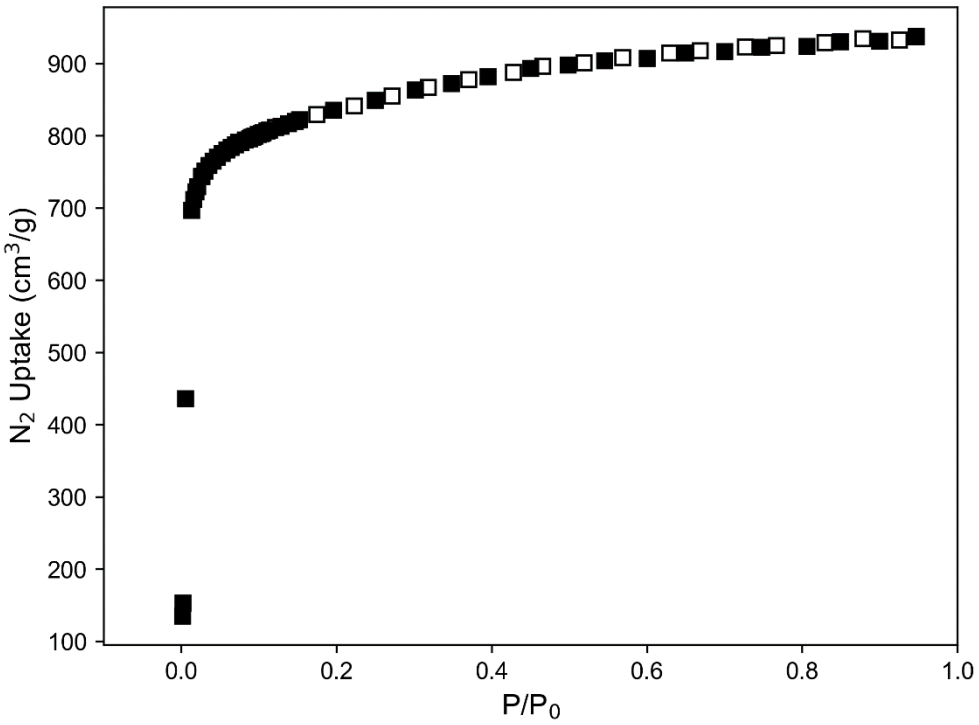

Figure S12. N_2 sorption isotherm for MOF-5 synthesized in DEET.

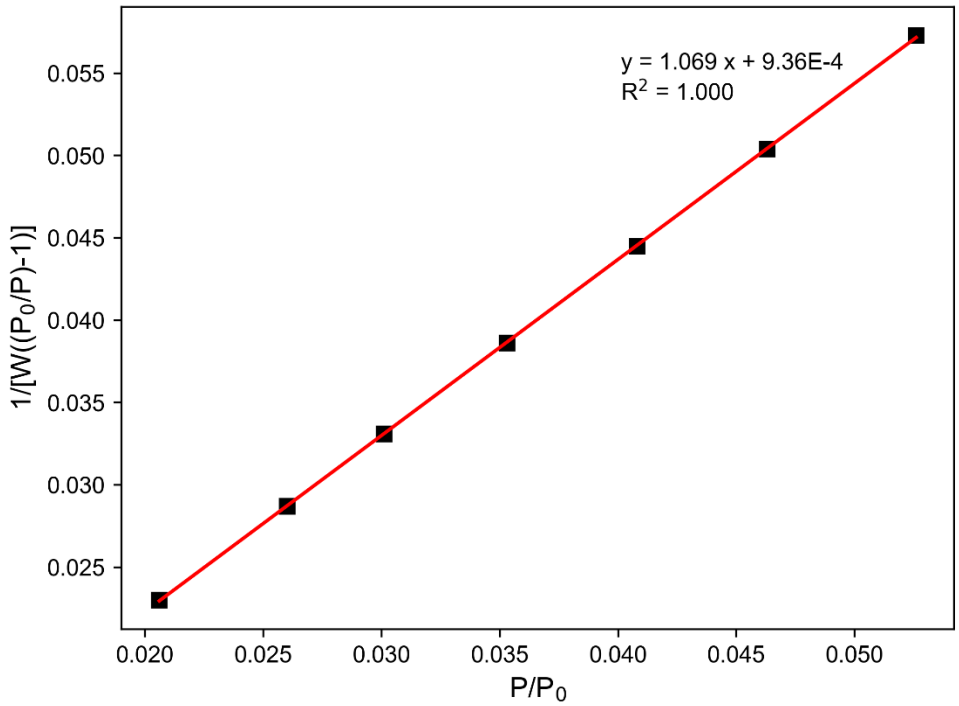

Figure S13. BET fit of isotherm data taken from MOF-5 synthesized in DEET.

6. Optical microscopy

MOF morphology was assessed using a digital 3D microscope (Hirox RH-2000). Optical micrographs are given in Figures S14 – S19.

MOF-5:

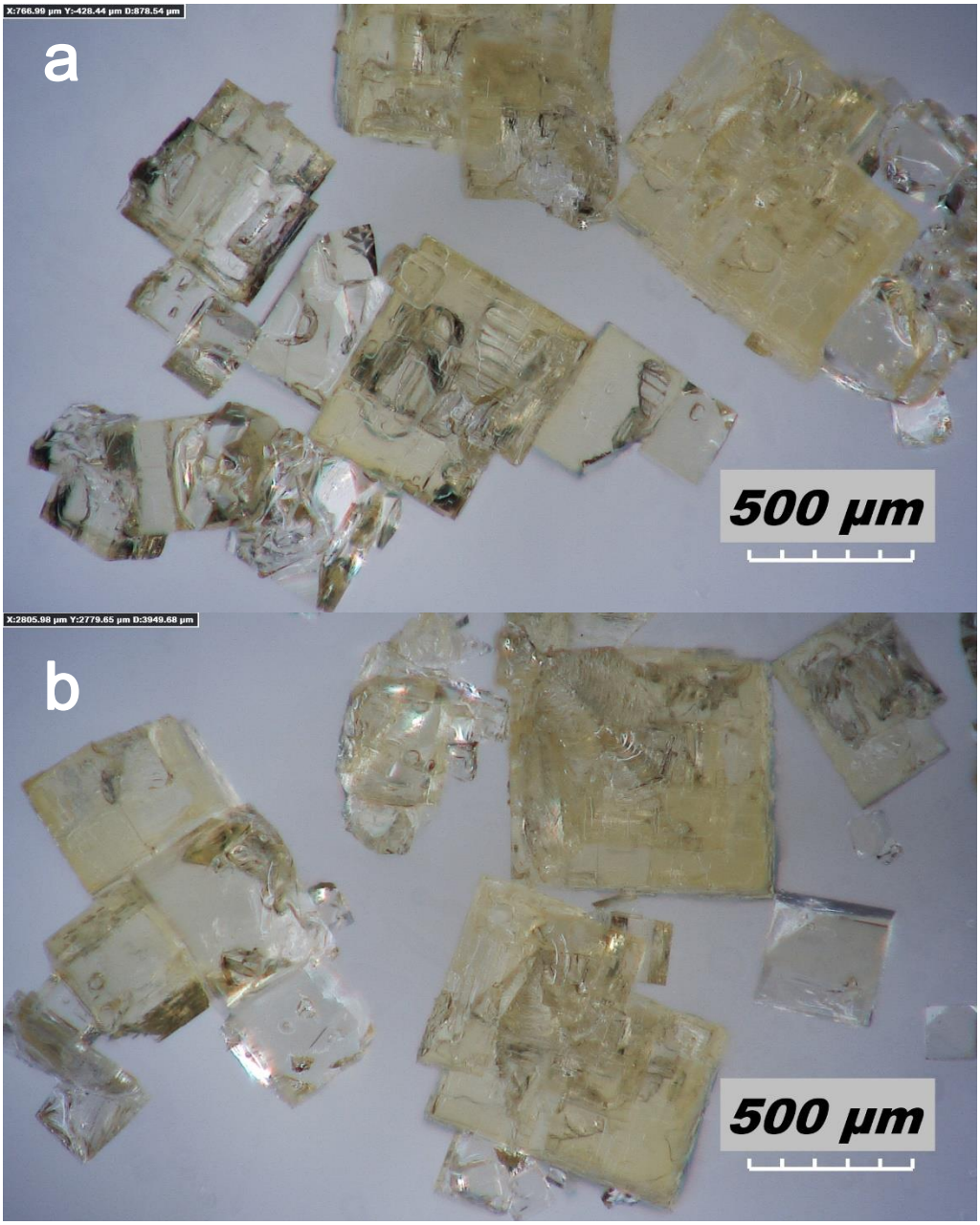

Figure S14. Optical micrographs of DEET-synthesized MOF-5 (a, b). The product shows the characteristic cubic morphology of the standard MOF-5 synthesis. Crystal sizes vary, but most are 200 – 600 µm in diameter.

UMCM-1:

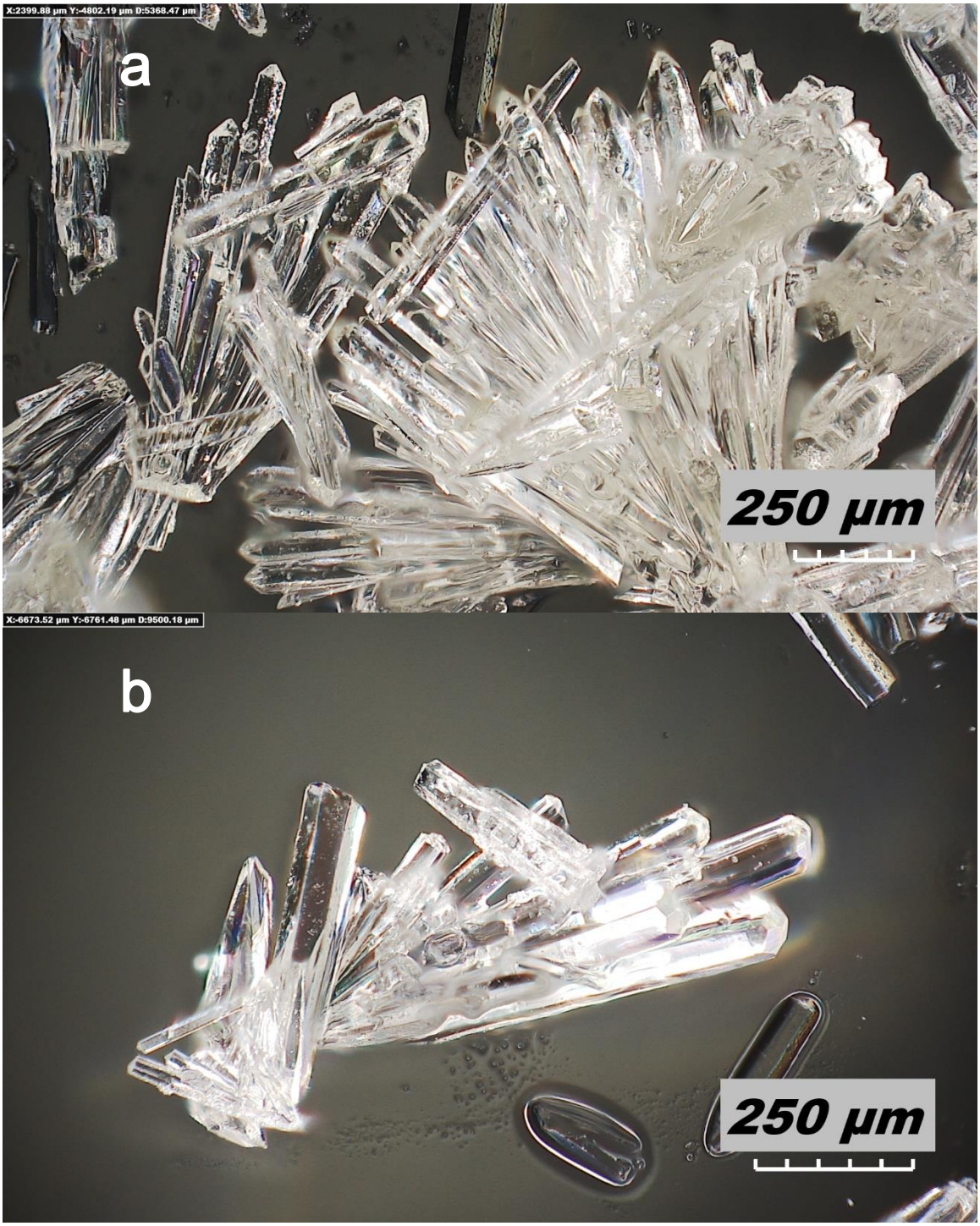

Figure S15. Optical micrographs of DEET-synthesized UMCM-1 (a, b). The product shows the characteristic needle morphology of the standard UMCM-1 synthesis. Crystals are as long as 1 mm, and range from 20 – 50 µm in diameter.

UMCM-9:

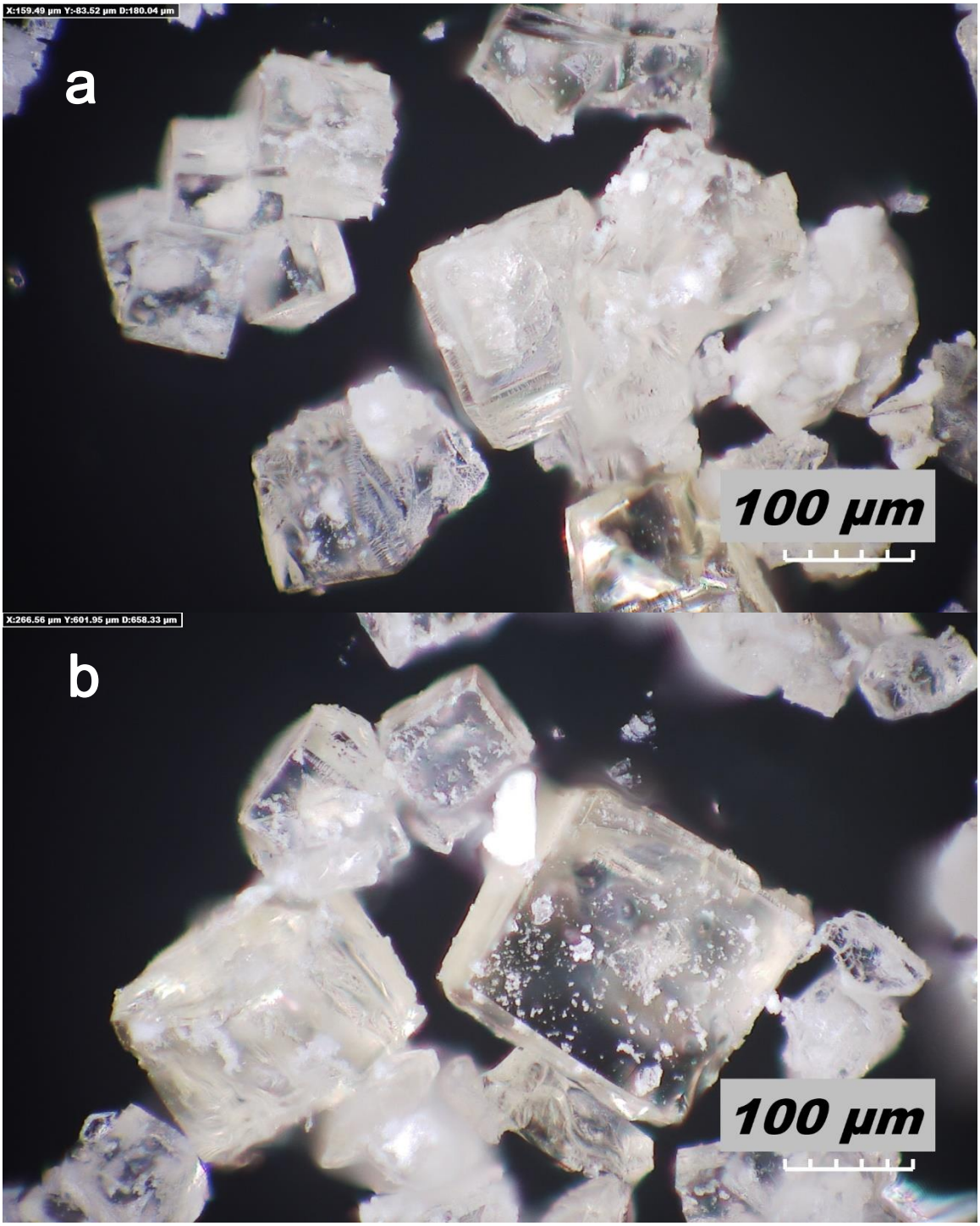

Figure S16. Optical micrographs of DEET-synthesized UMCM-9 (a, b). The product shows the characteristic cubic morphology of the standard UMCM-9 synthesis. Crystals are as large as ~250 µm in diameter, but most are closer to 100 µm.

MOF-177:

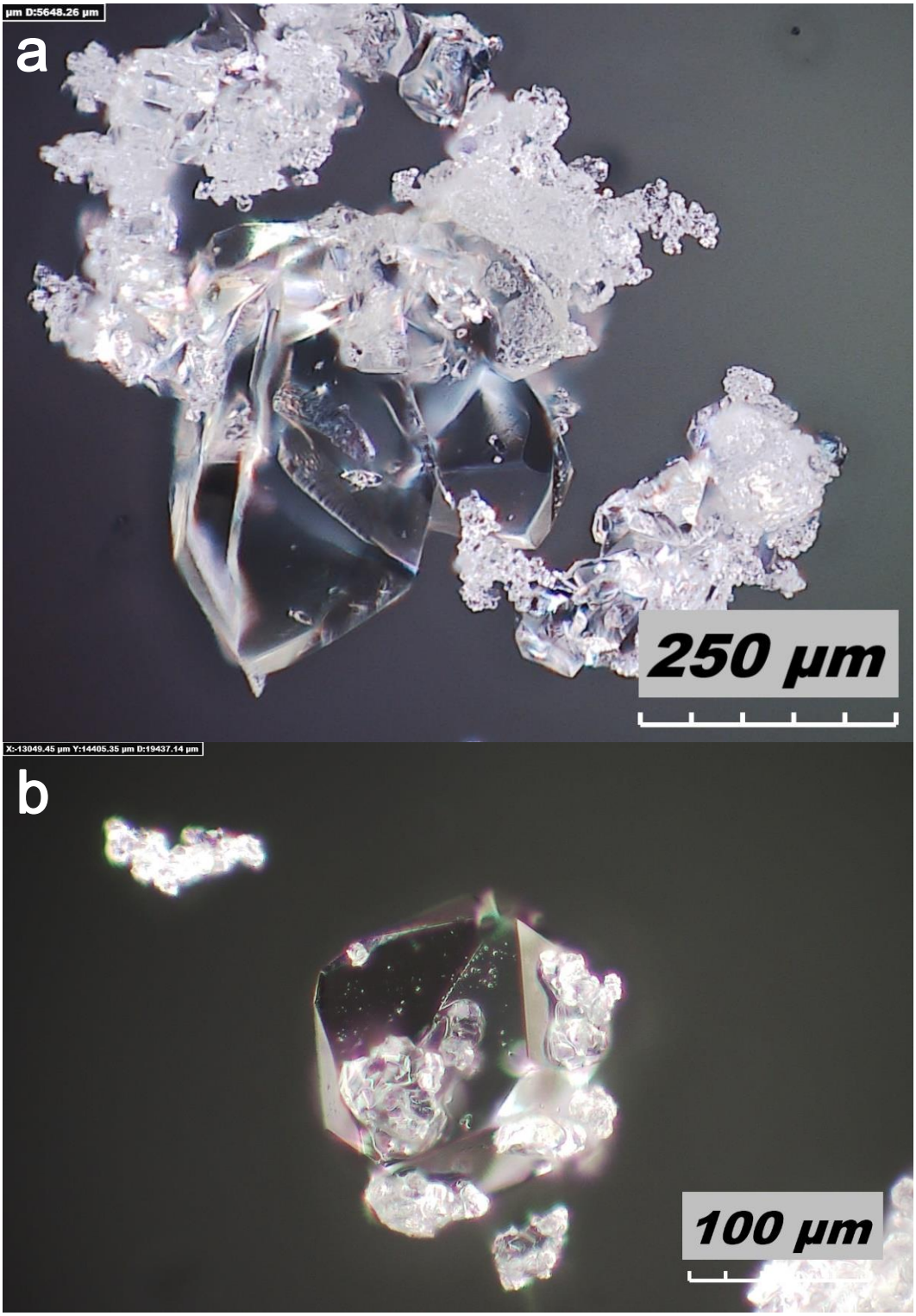

Figure S17. Optical micrographs of DEET-synthesized MOF-177 (a, b). Crystals appear blocky and occasionally octahedral, as the DMF-synthesis characteristically yields. Crystals are as large as ~200 µm in diameter, but most are closer to 10 – 50 µm range.

Zn/btc:

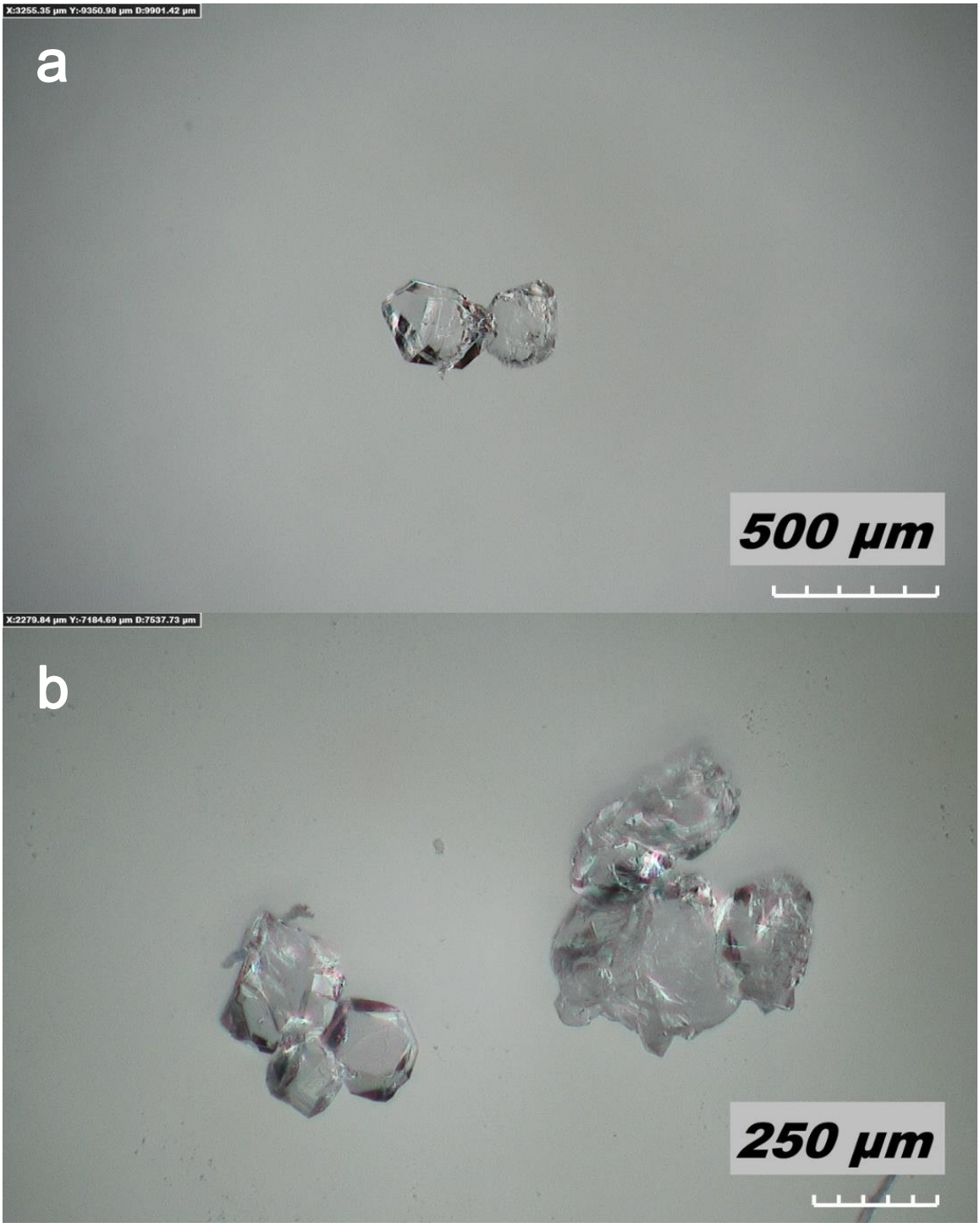

Figure S18. Optical micrographs of DEET-synthesized Zn/btc (a, b). The observed crystals have irregular/blocky morphologies. Crystals are 100 – 300 µm in diameter.

MOF-519:

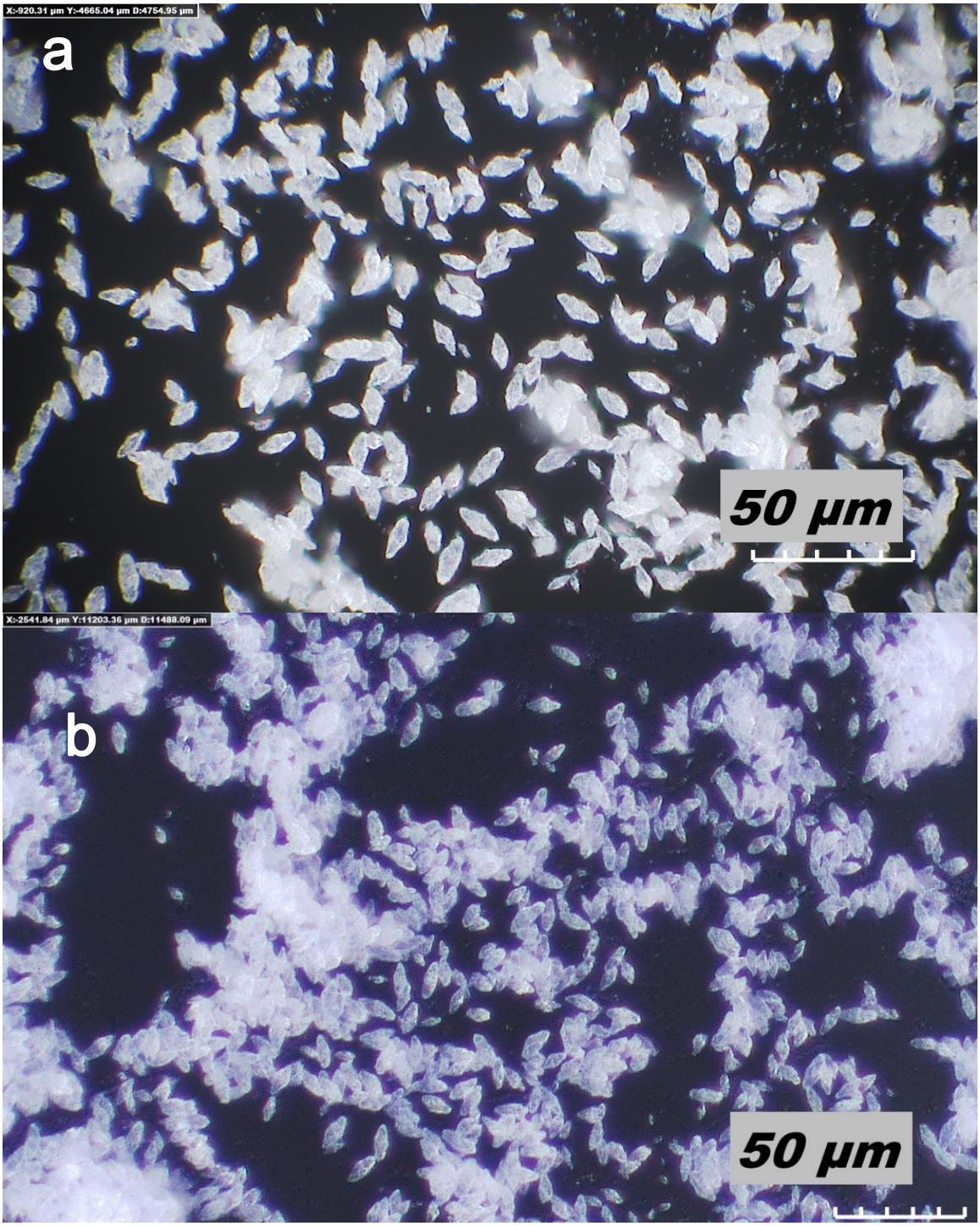

Figure S19. Optical micrographs of DEET-synthesized MOF-519 (a) and DMF-synthesized MOF-519 (b). Both syntheses yield crystals which appear to be elongated octahedra (approximately 5 × 5 × 10 µm).

7. Scanning electron microscopy

A JEOL JSM-7800FLV scanning electron microscope operating with an accelerating voltage of 10 kV was used to determine MOF morphology when morphology could not be determined by optical microscopy (HKUST-1, Cu/bdc). No images suitable for morphological identification could be collected for MIL-53(Al).

HKUST-1:

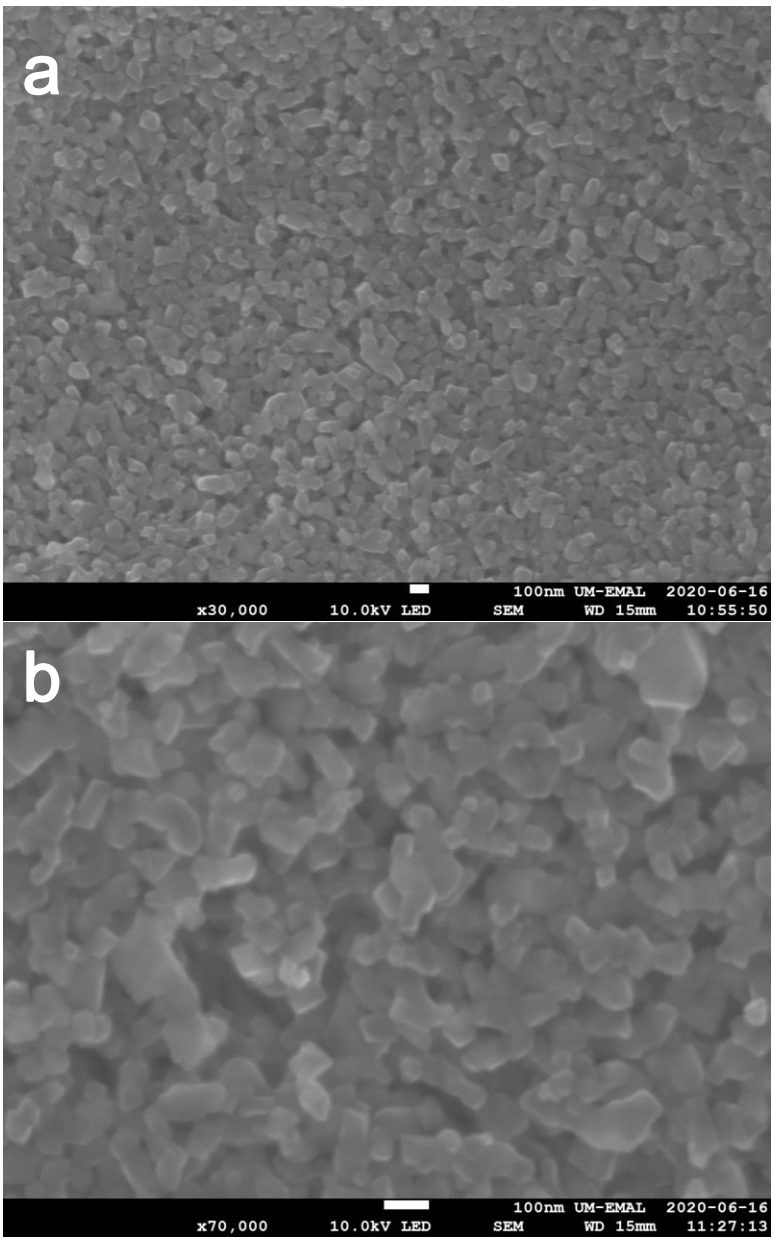

Figure S20. Scanning electron micrographs of DEET-synthesized HKUST-1 (a, b). Intergrown blocky crystals with sharp corners and flat faces are observed, with diameters generally ranging between 50 – 100 nm

Cu/bdc:

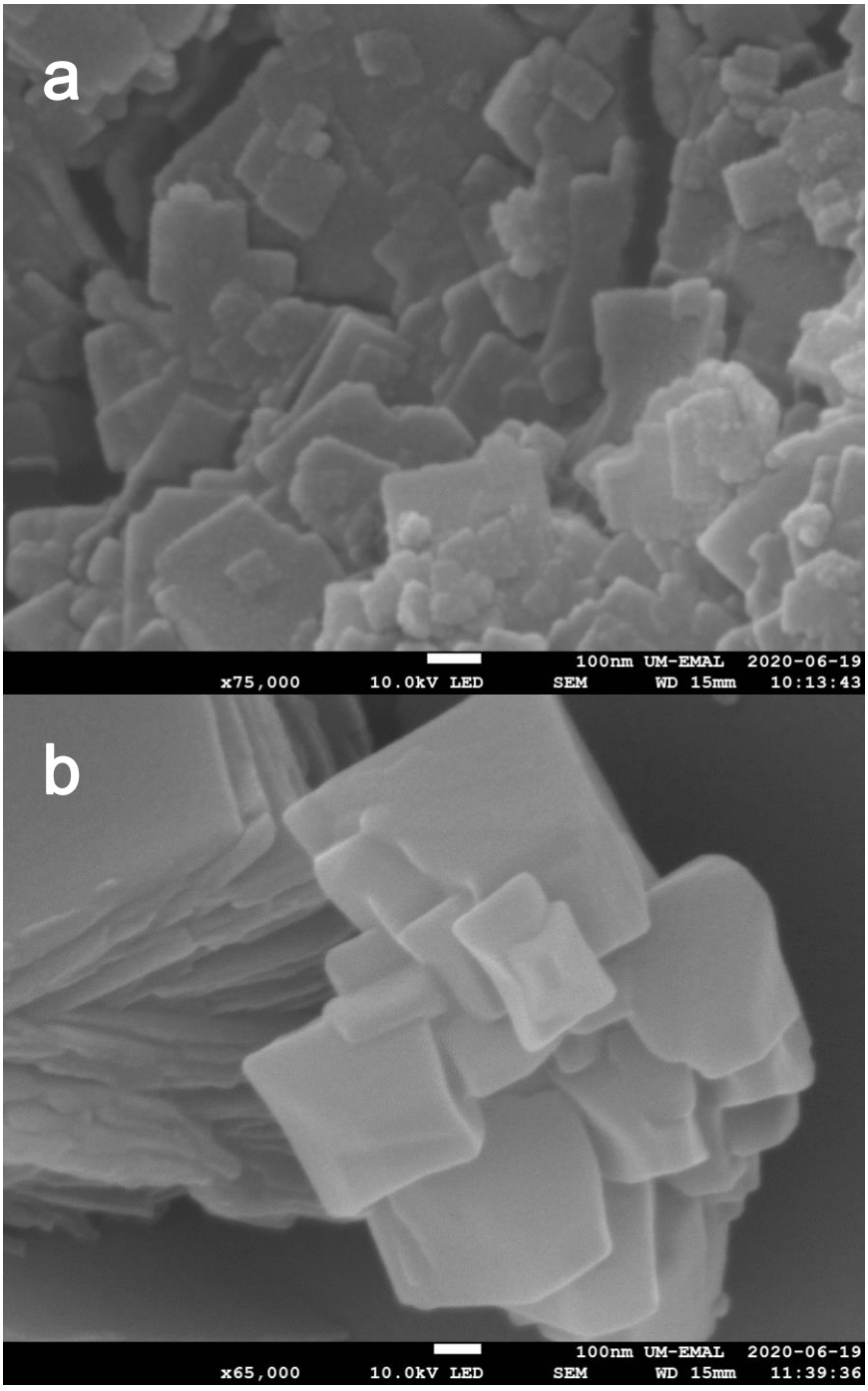

Figure S21. Scanning electron micrographs of DEET-synthesized Cu/bdc (a) and DMF-synthesized MOF-2 (b). Both appear to be stacked, intergrown plates.

8. ^{1}H-NMR

~10 mg of activated DEET-synthesized MOF-5 was digested using 35% DCl in D_2O (100 µL), then diluted with DMSO-d_6 (500 µL). ^{1}H-NMR measurement was performed at room temperature on a Varian Inova 500 spectrometer operating at 500 MHz. 16 scans with 2 second acquisition and a 1 second relaxation delay were collected.

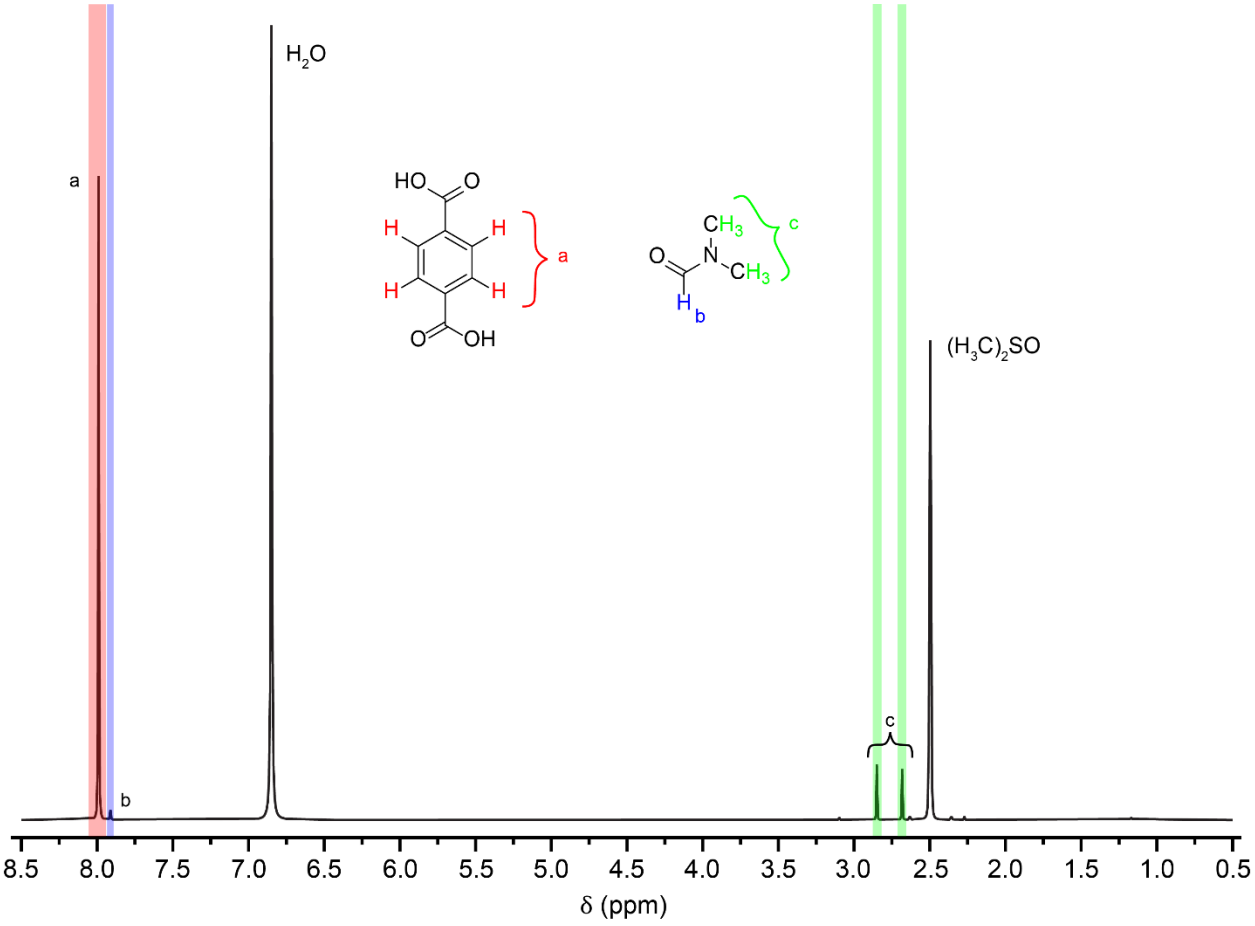

Figure S22. ^{1}H NMR spectrum of digested DEET-synthesized MOF-5 after solvent exchange and activation. Translucent colored overlays are for labelling only, the actual integration boundaries are given in Table S3. No DEET is observed in the solution.

Table S3. Chemical shifts, integral boundaries, integrals, and assignments for peaks in Figure S22, normalized to 100 bdc linkers (thus 400 bdc (H_a) protons).

Chemical shift (ppm)	Integration boundaries (ppm)	Integral (protons)	Assignment
7.99	8.113 – 7.937	400.00	Terephthalic acid
7.92	7.936 – 7.858	9.16	DMF formamide proton
2.85	2.899 – 2.798	34.16	DMF methyl group
2.69	2.715 – 2.656	32.31	DMF methyl group

Using DMF methyl groups (H_c) we can calculate a ratio of 1:0.11 between the amount of linker and DMF in the MOF. Per 100 bdc molecules:

$$32.31 + 34.16 = 66.47 \text{ total } \mathrm{H}_c \text{ integral}$$

$$\frac{66.47 \text{ DMF methyl protons}}{100 \text{ linkers}} \times \frac{1 \text{ DMF molecule}}{6 \text{ methyl protons}} = \frac{0.11 \text{ DMF molecules}}{\text{linker}}$$

8. References

1 H. Li, M. Eddaoudi, M. O'Keeffe and O. M. Yaghi, *Nature*, 1999, **402**, 276–279.
2 M. Eddaoudi, J. Kim, N. Rosi, D. Vodak, J. Wachter, M. O'Keeffe and O. M. Yaghi, *Science*, 2002, **295**, 469–472.
3 K. Koh, A. G. Wong-Foy and A. J. Matzger, *Angew. Chem. Int. Ed.*, 2008, **47**, 677–680.
4 K. Koh, J. D. Van Oosterhout, S. Roy, A. G. Wong-Foy and A. J. Matzger, *Chem. Sci.*, 2012, **3**, 2429.
5 H. Furukawa, M. A. Miller and O. M. Yaghi, *J. Mater. Chem.*, 2007, **17**, 3197–3204.
6 Q. Fang, G. S. Zhu, M. Xin, D. Zhang, X. Shi, G. Wu, G. Tian, L. Tang, M. Xue and S. L. Qiu, *Chem. J. Chinese U.*, 2004, **25**, 1016–1018.
7 K. S. Park, Z. Ni, A. P. Cote, J. Y. Choi, R. Huang, F. J. Uribe-Romo, H. K. Chae, M. O'Keeffe and O. M. Yaghi, *Proc. Natl. Acad. Sci.*, 2006, **103**, 10186–10191.
8 R. Banerjee, H. Furukawa, D. Britt, C. Knobler, M. O'Keeffe and O. M. Yaghi, *J. Am. Chem. Soc.*, 2009, **131**, 3875–3877.
9 D. Han, F.-L. Jiang, M.-Y. Wu, L. Chen, Q.-H. Chen and M.-C. Hong, *ChemComm*, 2011, **47**, 9861.
10 S. S. Y. Chui, S. M. F. Lo, J. P. H. Charmant, A. G. Orpen and I. D. Williams, *Science*, **283**, 1999, 1148–1150.
11 C. G. Carson, K. Hardcastle, J. Schwartz, X. Liu, C. Hoffmann, R. A. Gerhardt and R. Tannenbaum, *Eur. J. Inorg. Chem.*, 2009, **2009**, 2338–2343.
12 M. J. Katz, Z. J. Brown, Y. J. Colon, P. W. Siu, K. A. Scheidt, R. Q. Snurr, J. T. Hupp and O. K. Farha, *ChemComm*, 2013, **49**, 9449–9451.
13 V. Bon, I. Senkovska, M. S. Weiss and S. Kaskel, *CrystEngComm*, 2013, **15**, 9572.
14 W. P. Mounfield and K. S. Walton, *J. Colloid Interf. Sci.*, 2015, **447**, 33–39.
15 F. Gándara, H. Furukawa, S. Lee and O. M. Yaghi, *J. Am. Chem. Soc.*, 2014, **136**, 5271–5274.
16 T. H. Swan and E. Mack, *J. Am. Chem. Soc.*, 1925, **47**, 2112–2116.